

# ChemComm

Accepted Manuscript



This is an *Accepted Manuscript*, which has been through the Royal Society of Chemistry peer review process and has been accepted for publication.

*Accepted Manuscripts* are published online shortly after acceptance, before technical editing, formatting and proof reading. Using this free service, authors can make their results available to the community, in citable form, before we publish the edited article. We will replace this *Accepted Manuscript* with the edited and formatted *Advance Article* as soon as it is available.

You can find more information about *Accepted Manuscripts* in the [Information for Authors](#).

Please note that technical editing may introduce minor changes to the text and/or graphics, which may alter content. The journal's standard [Terms & Conditions](#) and the [Ethical guidelines](#) still apply. In no event shall the Royal Society of Chemistry be held responsible for any errors or omissions in this *Accepted Manuscript* or any consequences arising from the use of any information it contains.

## COMMUNICATION

## Gels and Threads: Mussel-inspired One-pot Route to Advanced Responsive Materials

Cite this: DOI: 10.1039/x0xx00000x

M. Krogsgaard, A. Andersen and H. Birkedal

Received 00th January 2012,  
Accepted 00th January 2012

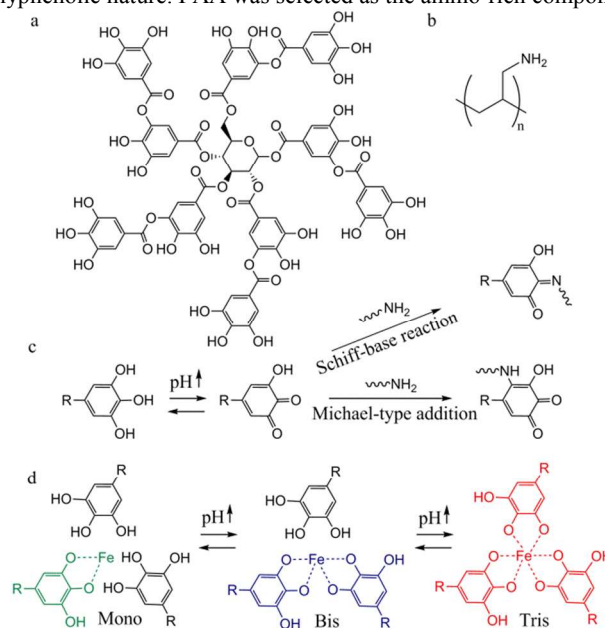
DOI: 10.1039/x0xx00000x

www.rsc.org/

**An inexpensive one-pot route to self-healing hydrogels with pH-tunable strength is presented. Hydrogels were formed by reacting tannic acid, trivalent metal ions and polyallylamine. Below pH 8 the hydrogels were supramolecular while above, covalent cross-linking strengthened the hydrogels. From concentrated mixtures, threads were spun, acting as water sensitive mechanical locks.**

Responsive<sup>1-4</sup> and self-healing<sup>5</sup> materials have a wide range of potential uses. Recently, a lot of effort has been put into the research of mussel-inspired hydrogels<sup>6</sup>. These hydrogels have been found to display interesting adhesive, self-healing and pH-responsive properties, which makes them attractive candidates for a wide range of biomedical applications. They make use of the multifaceted nature of catechols, such as DOPA used in the blue mussel byssus,<sup>6</sup> namely the ability to undergo covalent cross-linking at pH above 8<sup>7, 8</sup> or metal-mediated hydrogelation through coordination chemistry yielding self-healing hydrogels<sup>9-12</sup>. So far, these mussel-inspired hydrogels have been created using two-step processes. Here the catechol functionalities were initially incorporated into polymer backbones using various chemical reactions and thereafter these functionalized polymers were cross-linked to form 3D hydrogel networks either through catechol:Fe<sup>III</sup> coordination bonds or by the formation of covalent cross-links as a result of the oxidation of the catechol moiety. The blue mussel byssus features a range of proteins<sup>6</sup>. The adhesive proteins, Mfp-3 and Mfp-5, are rich in DOPA and in lysine, i.e. they comprise catechols and amines. We previously harnessed this information to develop g-DOPA-polyallylamine polymers that by reaction with Fe<sup>III</sup> resulted in self-healing hydrogels with a highly pH-dependent strength<sup>11</sup>. This method demanded grafting DOPA onto the polymer, a relatively simple step that nevertheless is time-consuming and requires expensive chemicals. Herein, we present a very simple, rapid and low-cost one-pot recipe for creating self-healing pH-responsive hydrogels inspired by the adhesive system of the blue mussel. This method is based on the low-cost natural polyphenol tannic acid (TA, Scheme 1a), which spontaneously becomes cross-linked into

hydrogels by iron ions and polyallylamine (PAA, Scheme 1b) as the pH is increased to above pH 3 (Scheme 1c and d). TA and PAA together act as models for the catechol and lysine-rich Mfp-3 and 5. TA is a member of the class of polyphenols that similarly to catechols<sup>6, 8</sup> has been shown to make coatings by covalent cross-linking<sup>13</sup> or by coordination with Fe<sup>III</sup><sup>14</sup>. The large number of pyrogallol groups on TA emulates the mussel foot protein's polyphenolic nature. PAA was selected as the amino-rich component



Scheme 1. The chemical structure of (a) tannic acid (TA) and (b) polyallylamine (PAA). (c) pH-catalyzed oxidation of the pyrogallol groups of tannic acid and subsequent cross-linking reactions with the amines on polyallylamine. (d) pH-dependent transition of the stoichiometry of the TA:Fe<sup>III</sup> coordination bond. R represents the remainder of the TA molecule.

due to its high solubility, which makes it easy to work with and provides a simple proof-of-concept system. The one-pot approach is however not limited to PAA but also works with other cationic polymers such as polylysine (Supplementary materials (ESI), Figure S1b). In addition to hydrogels, we further show that flexible and lightweight fibers can be spun from the TA/PAA/M<sup>III</sup> based materials and that the strength of these fibers depends on their degree of hydration and pH.

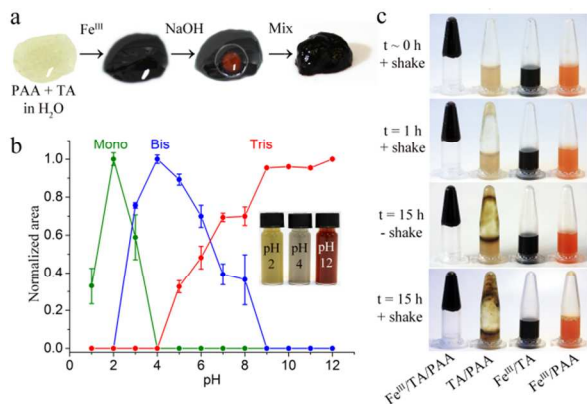


Figure 1. a) Hydrogel formation. b) Normalized area of the characteristic mono- (green), bis- (blue) and tris- (red) peaks plotted as a function of pH. The normalized areas were calculated from UV/VIS data and can be used as an estimate for the relative fractions of the different Fe<sup>III</sup>:pyrogallol coordination bonds (3:1 pyrogallol to Fe<sup>III</sup> ratio). The inserts show the color of the solutions at pH 2, 4 and 12 where the mono-, bis-, and tris- species prevail, respectively. To highlight the color the pH 4 and pH 12 solutions were diluted by a factor of 3 and 10, respectively. When no standard deviation can be seen, it is smaller than the size of the points. c) Photographs showing the physical state of the samples during the inverted-vial test (pH 8).

Self-healing hydrogels were created in a one-pot approach by mixing TA, PAA and Fe<sup>III</sup> ions at pH 1.5 and then increasing the pH to the desired value by the addition of NaOH (TA and PAA concentration of 14.7 mg/mL and 133 mg/mL, respectively, 3:1 pyrogallol to Fe<sup>III</sup> ratio). At pH 3 the material was a bluegreen liquid due to the abundance of mono- and bis-pyrogallato iron complexes, but as the pH was increased to above 3, the material transformed into a sticky blue/red solid due to the formation of bis- and tris- cross-links (Figure 1a). The pH-dependent assembly was investigated using UV/VIS spectroscopy on diluted solutions as the mono-, bis-, and tris-species display characteristic absorption bands in the visible range, which can be used to determine the abundance of the various species (ESI, Figure S5). The mono-, bis- and tris-species were found to prevail in the pH range 1-2, 3-6 and 7-12, respectively (Figure 1b). The fact that tris-species dominated all the way from pH 7 to 12 is different from systems involving DOPA functionalized polymers cross-linked by Fe<sup>III</sup><sup>9, 11</sup> but is in line with the observed transitions in Fe<sup>III</sup>/TA coatings by Caruso *et al.*<sup>14, 15</sup> and with other works employing more acidic DOPA analogues.<sup>12, 16</sup> This illustrates how the pH-dependent polymer cross-linking can be controlled by modifying the polyphenol used.

The importance of all three components, *i.e.* Fe<sup>III</sup>, TA and PAA, was investigated using inverted-vial tests (Figure 1c). Vials with combinations of the three were incubated at pH 8 for up to 15 h and the physical state of the materials assessed by shaking. A hydrogel formed instantaneously only when all three components were present. In contrast, mixtures of Fe<sup>III</sup> and TA remained a dark red liquid because the PAA polymer backbone is required to establish a

three-dimensional hydrogel network. The TA and PAA mixture was initially a liquid but slowly transformed to a gel after about 15 h. This gelation likely resulted from the slow formation of covalent cross-links as a result of oxidation of TA (Scheme 1c). This hypothesis is supported by the fact that the TA/PAA sample became darker as a function of time and the part of the sample exposed to air turned darker brown than the rest of the sample. The Fe<sup>III</sup> and PAA mixture remained a liquid throughout the experiment. These experiments proved that the cohesive polymer network in the hydrogels was established through a combination of hydrogen bonding and/or covalent cross-links between TA and PAA (Scheme 1c), and coordination bonds between TA and Fe<sup>III</sup> (Scheme 1d).

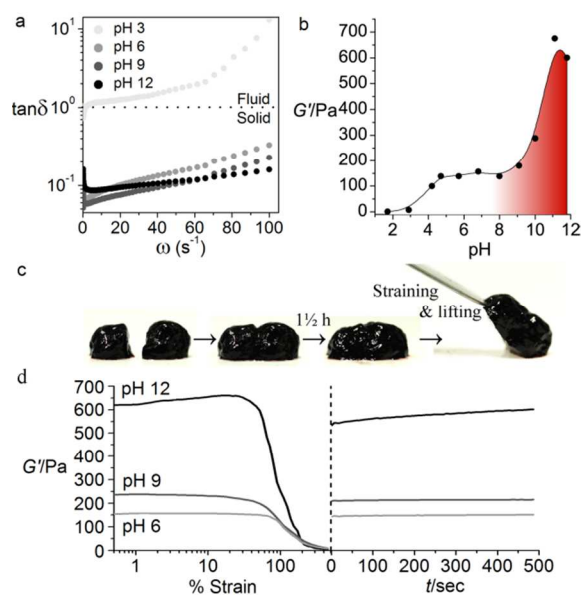


Figure 2. a) Loss tangent ( $\tan \delta$ ) plotted as a function of the angular frequency ( $\omega$ ) for four pH values. b) Storage modulus ( $G'$ ) plotted as a function of pH for a strain of 15% and an angular frequency of 25 s<sup>-1</sup>. The red color highlights the covalent contribution. c) Qualitative recovery test. d) Quantitative recovery test. Hydrogels with different final pH (pH 6, 9, and 12) were sheared using rheology at increasing strain and 1 s<sup>-1</sup> after which the recovery was monitored at 1% strain and 1 s<sup>-1</sup>.

The hydrogels are viscoelastic meaning that their behaviour lies between the classical extremes of an ideal solid and an ideal fluid. Dynamic oscillatory rheology was used to probe the viscoelastic properties of the hydrogels. The hydrogels were sheared between two parallel plates under increasing frequency (ESI). Figure 2a shows the frequency dependence of the loss tangent ( $\tan \delta$ ) for pH 3, 6, 9 and 12 materials (see associated moduli in Figure S6). At pH 3, viscous properties dominated over the elastic response. At pH 6, 9 and 12 hydrogels formed with the elastic properties dominating. The obtained storage modulus  $G'$  was plotted as a function of pH (Figure 2b) for a frequency of 25 s<sup>-1</sup> (similar behavior was obtained for other frequencies). The storage modulus depends quite strongly on pH. At pH below about 4, the samples were liquid. In the 4-8 pH-range, gels were observed with a maximum mechanical strength around 150 Pa. At such low pH values, gels can be expected to be formed from Fe<sup>III</sup> cross-linked TA moieties that form gel-supporting networks by non-covalent interactions with PAA. At pH above 8 the gel strength increased strongly, Figure 2b. We attribute this behavior to the formation of covalent TA-PAA bonds, Scheme 1c.

Contrary to the majority of covalent bonds, coordination bonds are reversible and impart self-healing properties to the hydrogels, meaning that they spontaneously repair after fracture<sup>9, 11</sup>. Initially, the self-healing properties were qualitatively tested by forcing a pH 8 hydrogel to fracture with a spatula (Figure 2c). Next, the hydrogel pieces were brought back together and allowed to reform the broken bonds. The hydrogel was found to recover its original shape within 1½ h. The self-healing properties were also investigated quantitatively using rheometry. Here, hydrogels were subjected to increasing strains until fracture and the recovery of the mechanical properties was monitored as a function of time (Figure 2d). The rate of recovery was found to depend on pH. Whereas the pH 6 and pH 9 hydrogels instantly recovered their original stiffness (Storage modulus  $G'$ , of ~150 and 230 Pa, respectively), the recovery at pH 12 was slower. Even after 500 s the original strength was not fully recovered. The reduced self-healing properties at pH 12 can be explained by the increasing number of irreversible covalent cross-links formed at high pH.<sup>9</sup> Support for this explanation was obtained from gel reversibility experiments involving competitive binding of  $\text{Fe}^{\text{III}}$  with EDTA (ESI, Figure S8). After 17 h the pH 6 gel had completely dissolved whereas the vials with the pH 9 and 12 gels still contained residual hydrogel material. The remaining material was a result of irreversible covalent cross-links formed between PAA and TA emphasizing that the hydrogels are held together by a combination of irreversible and reversible cross-links above pH 8 (Scheme 1c and d). The interplay between irreversible and reversible cross-links is highly pH-dependent; as the pH is increased above 8, the number of irreversible bonds is increased, resulting in limited gel reversibility and in enhanced mechanical strength (Figure 2b).

The supramolecular behavior in the system was further probed by Small Angle X-ray Scattering (SAXS, ESI).<sup>11</sup> The SAXS data showed that the combination of all three components lead to nanostructures that depend on pH and were distinctly different from those observed in pure PAA<sup>11</sup> or in  $\text{Fe}^{\text{III}}$ /TA (Figure S7). As pH was increased, scattering at low angles increased at the expense of higher angles. This indicates that larger nanostructures formed as pH was increased in agreement with the notion of the multicomponent cross-linking mechanisms outlined in Scheme 1.

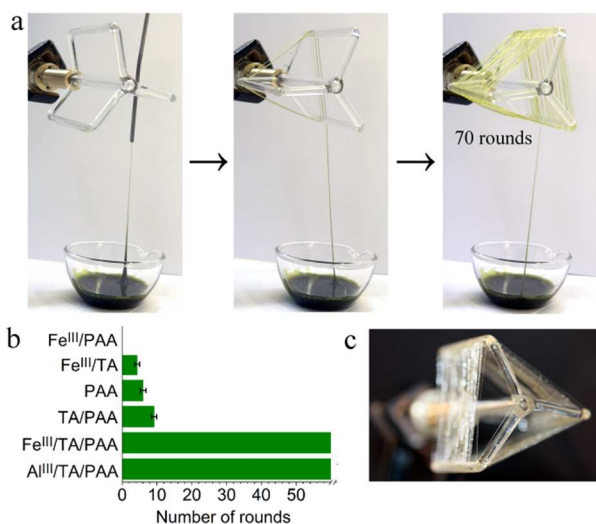


Figure 3. a) Threads spun from a  $\text{Fe}^{\text{III}}$ /TA/PAA mixture. The threads are green due to the abundance of the mono-species at pH 1. b) Histogram showing the number of rounds performed by the mill when exposed to combinations of  $\text{Fe}^{\text{III}}$ / $\text{Al}^{\text{III}}$ , TA and PAA ( $n = 10$ ). c) Transparent and colorless threads formed using  $\text{Al}^{\text{III}}$ .

The hydrogels discussed above had rather large water content and were thus only moderately good models for the solid thread formation seen in blue mussel byssi. At high concentration (15 times the concentration of the hydrogel recipe), a qualitatively different behavior was observed. At low pH (pH 1), a thick and sticky (as determined by inversion tests) substance was created that would easily attach to e.g. spatulae. More importantly, it was possible to harvest very long homogeneous threads from it (20 °C, < 45% humidity). This was achieved in several ways, here we present one inspired by the method used to extract drag-line silk fibers from spiders<sup>17</sup>. Threads were obtained using a three-blade glass mill driven by an electric motor. A seed thread was extracted manually from the  $\text{Fe}^{\text{III}}$ /TA/PAA mixture and attached by contact to the mill. Threads were spun on the mill by rotating the mill with the motor (rotation speed: 10-25 rpm) and laterally displacing the sample container (Figure 3a and supplementary material that displays a video of the process, V1). Several meter long threads could be obtained in this straightforward manner. Green threads were formed using  $\text{Fe}^{\text{III}}$  (Figure 3a); however according to the hard/soft acid/base principle threads and hydrogels will form when using other hard metal ions (Figure S1a). This design feature allows for the introduction of other metal ions. Indeed transparent and colorless threads were obtained using  $\text{Al}^{\text{III}}$  as metal source (Figure 3c).

The thread thickness could be varied very easily by controlling the pulling speed. The diameter of the threads was found to increase exponentially from  $39 \pm 6$  to  $280 \pm 50$   $\mu\text{m}$  when increasing the rotation speed from 10 to 25 rpm (Figure S2), reflecting the strongly non-Newtonian properties of the system. Meter-long threads were only obtained when all three components were present. When only one or two components were present, the number of rounds the mill could be turned before ‘thread’ fracture was very limited, typically below 10, as shown in Figure 3b. With the  $\text{M}^{\text{III}}$ /TA/PAA systems, no upper bound to the number of turns was found ( $\text{M}$ :  $\text{Fe}^{\text{III}}$ / $\text{Al}^{\text{III}}$ ); threads could be spun till exhaustion of the source material. SEM images showed that the thread surface was smooth (Figure S9).

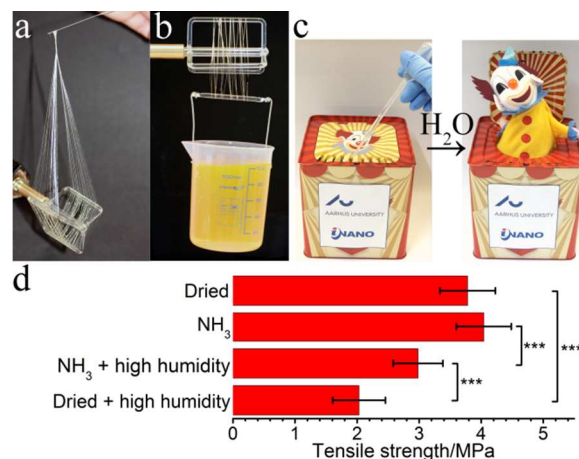


Figure 4. a) Extendable and flexible wet threads ( $\text{Al}^{\text{III}}$ /TA/PAA). b) 14 dry threads supporting a weight of 118 g ( $\text{Al}^{\text{III}}$ /TA/PAA). c) Jack-in-the-box kept closed by dry threads (left). When actuated by drops of water, the threads break and the clown pops out (right). d) Tensile strength of threads formed under different conditions ( $n = 17$ ). Stars indicate significance in two-tailed Student’s t-test; \*\*\* $P < 0.0005$ .

When loaded in the wet state, the threads deformed strongly and inelastically (Figure 4a). This inelastic deformation and non-Newtonian behavior is likely the origin of thread formation. Dried

threads were remarkably strong (Figure 4b and 4d). Threads could be broken by addition of water that made them swell (see SEM image in Figure S9) and exit the high-concentration thread-forming concentration regime. This is illustrated in Figure 4c and in the video V2 where a children's toy was kept tightly closed by threads. Subsequently the box was opened by swelling the threads locally with a drop of water; revealing the clown inside.

The sensitivity of the threads towards humidity was investigated by monitoring the mass gain of a dried thread as a function of time at 45% humidity (ESI, Figure S3). The experiments showed that the threads increase their mass by 15-25% of their original mass within ~20 minutes. The tensile strengths of the threads were quantified by loading them as shown in Figure S4. The tensile strength could then be estimated from the measured yield loads (ESI). The experiment was conducted under the following conditions to test the influence of humidity and pH on the tensile strength: *i*) at low humidity (40% humidity, 20 °C), *ii*) after NH<sub>3</sub> gas exposure to increase pH and *iii*) after one of the aforementioned conditions followed by high humidity (90% humidity, 25°C). Upon ammonia exposure, the threads changed color from green to dark red as a consequence of the pH increase. The resulting data is depicted in Figure 4d. Dry threads show a tendency to be slightly reinforced upon pH increase though the effect is only significant within a 90 % confidence interval. The slight increase in the strength at high pH can be explained by the formation of bis- and tris- Fe<sup>III</sup>-pyrogallol complexes together with contributions from covalent cross-linking (Scheme 1c and d). The threads are weakened at high humidity regardless of the precondition. The threads exposed to NH<sub>3</sub> prior to high humidity are however more resistant to swelling than the fibers that have only been dried. This can be understood from the fact that dry threads are held together by strong ionic and/or hydrogen bond interactions that weaken considerably upon exposure to water vapour. At high pH, this effect is hampered by covalent cross links, which rescues a significant part, about 50%, of the swelling induced weakening.

## Conclusions

We have shown how self-healing and pH-responsive hydrogels with a remarkable set of easily adjustable properties can be created in a simpler and low-cost on-pot route compared to previous mussel-inspired hydrogels<sup>9-12</sup>. The tensile strength of the dried water-responsive fiber materials, 3.8±0.4 MPa, is ~1% of the strength of cotton.<sup>18</sup> We believe that this straight-forward approach to mussel-inspired materials facilitates their use in a range of applications such as triggered response systems.

Funding from the Human Frontiers Science Program (HFSP), the Carlsberg Foundation, the Lundbeck Foundation and the Danish Council for Independent Research | Technology and Production Sciences is gratefully acknowledged.

## Notes and references

<sup>a</sup>Department of Chemistry and iNANO, Gustav Wieds Vej 14, DK-8000 Aarhus, Denmark. Corresponding Author: HB. Fax: (-45) 86196199. Email: hbirkedal@chem.au.dk

Electronic Supplementary Information (ESI) available: Experimental procedures and materials characterization, Figures S1-S9 and videos V1-V2. See DOI: 10.1039/c000000x/

1. E. S. Gil and S. M. Hudson, *Prog. Polym. Sci.*, 2004, **29**, 1173-1222.
2. R. J. Mart, R. D. Osborne, M. D. Stevens and R. V. Ulijn, *Soft Matter*, 2006, **2**, 822.
3. D. Roy, J. N. Cambre and B. S. Sumerlin, *Prog. Polym. Sci.*, 2010, **35**, 278.

4. M. A. Cohen Stuart, W. T. S. Huck, J. Genzer, M. Müller, C. Ober, M. Stamm, G. B. Sukhorukov, I. Szleifer, V. V. Tsukruk and M. Urban, *Nature Materials*, 2010, **9**, 101.
5. M. D. Hager, P. Greil, C. Leyens, S. van der Zwaag and U. S. Schubert, *Adv. Mater.*, 2010, **22**, 5424.
6. B. P. Lee, P. B. Messersmith, J. N. Israelachvili and J. H. Waite, *Annu. Rev. Mater. Res.*, 2011, **41**, 99.
7. H. Lee, S. M. Dellatore, W. M. Miller and P. B. Messersmith, *Science*, 2007, **318**, 426.
8. M. E. Lyngø, R. van der Westen, A. Postma and B. Stadler, *Nanoscale*, 2011, **3**, 4916.
9. N. Holtén-Andersen, M. J. Harrington, H. Birkedal, B. P. Lee, P. B. Messersmith, K. Y. C. Lee and J. H. Waite, *PNAS*, 2011, **108**, 2651.
10. Z. Shafiq, J. Cui, L. Pastor-Pérez, V. San Miguel, r. A. Gropeanu, C. Serrano and A. del Campo, *Angew. Chem. Int. Ed.*, 2012, **51**, 4332.
11. M. Krogsgaard, M. A. Behrens, J. S. Pedersen and H. Birkedal, *Biomacromolecules*, 2013, **14**, 297.
12. M. S. Menyo, C. J. Hawker and J. H. Waite, *Soft Matter*, 2013, **9**, 10314.
13. T. S. Sileika, D. G. Barrett, R. Zhang, K. H. A. Lau and P. B. Messersmith, *Angew. Chem. Int. Ed.*, 2013, **52**, 10766.
14. H. Ejima, J. J. Richardson, K. Liang, J. P. Best, M. P. van Koevorden, G. K. Such, J. Cui and F. Caruso, *Science*, 2013, **341**, 154.
15. J. Guo, Y. Ping, H. Ejima, K. Alt, M. Meissner, J. J. Richardson, Y. Yan, K. Peter, D. von Elverfeldt, C. E. Hagemeyer and F. Caruso, *Angew. Chem. Int. Ed.*, 2014, **53**, 5546.
16. L. García-Fernández, J. Cui, C. Serrano, Z. Shafiq, R. A. Gropeanu, V. San Miguel, J. I. Ramos, M. Wang, G. K. Auernhammer, S. Ritz, A. A. Golriz, R. Berger, M. Wagner and A. del Campo, *Adv. Mater.*, 2012, **25**, 529.
17. R. W. Work and P. D. Emerson, *J. Arachnol.*, 1982, **10**, 1.
18. P. Wambua, J. Ivens and I. Verpoest, *Comp. Sci. Tech.*, 2003, **63**, 1259.

## COMMUNICATION

## TABLE OF CONTENTS GRAPHIC:

Self-healing hydrogels are obtained in a one-pot reaction between tannic acid, trivalent metal ion and polyallylamine. At high concentrations, meter-long threads could be drawn from low pH solutions (see photograph).

